

DYNAMIC MAGNETOCONDUCTIVITY FOR AN ELECTRON-IMPURITY
SYSTEM

STRONG COUPLING CASE*

BY C. C. CHEN

Department of Physics, Ohio University, Athens, Ohio, USA

AND S. FUJITA

Department of Physics and Astronomy, State University of New York at Buffalo, New York**

(Received July 25, 1968)

The rigorous analysis of the contribution of one-electron-one-impurity interaction process to the dynamic magnetoconductivity $\sigma(\omega, B)$ is carried out by means of correlation function formula (Kubo's formula) and the connected diagram expansion. It is shown that this contribution is completely described in terms of the generalization of the transition matrix on- and off-energy shell.

1. Introduction

The dynamic response of a system to a time-dependent external field is in general more complicated than the static response. Firstly any interaction mechanism will yield complex number contribution to the coefficients of the dynamic response. Secondly in contrast to the static case the contribution of even the binary (one electron and one impurity) collision process can not be expressed in terms of the scattering cross-section alone. These points have been explicitly demonstrated for the weakly coupled electron-impurity system in the previous paper [1].

In an earlier paper [2] by starting with Kubo's current correlation formula [3] for the conductivity and by analyzing it in terms of connected diagrams, it was established that the dynamic magnetoconductivity $\sigma(\omega, B)$ as a function of an arbitrary frequency ω of the electric field and an arbitrary constant magnetic field B can be rigorously calculated

* Research sponsored by the Air Force Office of Scientific Research, Office of Aerospace Research, United States Air Force, under AFOSR Grant Nr 854-65.

** Address: Department of Physics and Astronomy, State University of New York at Buffalo, Buffalo, New York 14214, USA.

from a single transport equation. See (2.4) and (2.6). An important advantage of this approach is that one can clearly identify the contribution of the one-electron-one-impurity interaction process to $\sigma(\omega, B)$. We believe that the identification of this contribution and its rigorous analysis has never been done before, although the corresponding contribution to the static conductivity of a magnetic field-free system ($\omega = 0, B = 0$) was discussed earlier in their classic paper by Kohn and Luttinger [4].

In the present article this contribution for an arbitrary strong potential will be investigated in detail. In particular it will be shown that this one-electron-one-impurity contribution to the dynamic magnetoconductivity $\sigma(\omega, B)$ can be rigorously described in terms of a generalization of the transition matrix on- and off-energy shell.

In Section 2 the method of connected diagrams [2], by which Kubo's correlation function formula for the conductivity [3] can be calculated in a systematic manner, is summarized. In Section 3 the contribution of one-electron-one-impurity processes to the dynamic magnetoconductivity $\sigma(\omega, B)$ is defined in terms of connected diagrams.

A connected diagram is defined in terms of Liouville operators which generate commutators upon acting on a density operator. The actual calculation of the matrix elements of diagram contributions can be facilitated with aid of *c*-number diagrams [5]. This is discussed in Section 4. It is shown in Section 5 that the contribution of the one-impurity process is completely described in terms of the generalized transition matrices off the energy shell ($t_{\lambda\nu}(\mu): \lambda \neq \mu, \nu \neq \mu$) as well as those on the energy shell ($t_{\nu\lambda}(\mu):$ either of $(\lambda, \nu) = \mu$).

The general results are expressed in terms of the solutions of the integral equations. Although the solutions to these equations are difficult to obtain, a number of simple limiting cases can be worked out by introducing approximations, and will be reported in separate papers.

2. Method of connected diagram analysis

Let us consider an electron-impurity system characterized by the time-independent Hamiltonian

$$\begin{aligned} H &\equiv \sum_j h^{(j)} \\ &\equiv \sum_j h_0^{(j)} + \lambda \sum_{j, \alpha} \tilde{v}_\alpha^{(j)}, \end{aligned} \quad (2.1)$$

where $h_0^{(j)}$ stands for the kinetic energy of *j*-th electron, which may contain the energy due to a constant magnetic field; $\tilde{v}_\alpha^{(j)} \equiv \tilde{v}(r^{(j)} - R_\alpha)$ for the potential energy due to the impurity α at R_α ; λ is the coupling constant.

When the Hamiltonian is composed of single-particle energies as in (2-1), Kubo's formula [3] for the electrical conductivity can be expressed in terms of single-particle trace, denoted by tr , as [5]

$$\sigma_{rs}(\omega) = \int_0^\infty dt e^{-i\omega t} \lim_{\Omega \rightarrow 0} \Omega^{-1} \frac{\partial}{\partial u_s} \text{tr} \{ j_r e^{-i\hbar n' e^{i\hbar t}} \} \quad (2.2)$$

$$n' \equiv [e^{\beta(\hbar - j \cdot u - \epsilon)} + 1]^{-1}, \quad (2.3)$$

where j_r is the r -component of the velocity operator multiplied by the electronic charge $-e$, and u is a c -number vector; the u_s -derivate is to be evaluated at $u = 0$, and this convention will be used implicitly throughout the text.

According to the connected diagram analysis [2] the conductivity $\sigma_{rs}(\omega)$ can be alternatively calculated by

$$\sigma_{rs}(\omega) = -i \lim_{a \rightarrow 0} \text{tr} \{j_r \psi_s(-\omega + ia)\} \quad (2.4)$$

$$\psi_s(z) \equiv \frac{\partial n'_z}{\partial u_s} \equiv i \int_0^\infty dt e^{izt} \frac{\partial n'}{\partial u_s}, \quad (2.5)$$

where the operator $\psi \equiv (\psi_x, \psi_y, \psi_z)$ is found to satisfy the transport equation

$$(z - h_0)\psi(z) + \frac{\partial n'^{(c)}}{\partial u} + \left(f_z \frac{\partial n'}{\partial u}\right)^{(c)} = -g_z \psi(z) \quad (2.6)$$

$$g_z \equiv [-\lambda v + \lambda^2 v R_z^{(0)} v - \lambda^3 v R_z^{(0)} v R_z^{(0)} v + \dots]^{(c)}$$

$$f_z \equiv -\lambda v R_z$$

$$R_z \equiv [h - z]^{-1} = R_z^{(0)} - \lambda R_z^{(0)} v R_z^{(0)} + \dots$$

$$R_z^{(0)} \equiv [h_0 - z]^{-1}. \quad (2.7)$$

In these expressions, the script letters h , h_0 and v are defined such that

$$hn' \equiv [h, n'] \equiv hn' - n'h \quad (2.8)$$

and the superscript (c) means the restriction that the product should contain no free line segments in the diagram language, *e.g.*

$$(v R_z^{(0)} v)^{(c)} \equiv n_s \int d^3 R_\alpha \tilde{v}_\alpha R_z^{(0)} \tilde{v}_\alpha + \frac{1}{2} n_s^2 \iint d^3 R_\alpha d^3 R_\beta \tilde{v}_\alpha R_z^{(0)} \tilde{v}_\beta \chi_2(R_\alpha - R_\beta),$$

where $\chi_2(R_\alpha - R_\beta)$ is the two-impurity correlation function.

A connected diagram is composed of non-free particle line segments, potential and correlation bonds. A particle line is called free or non-free according to whether the diagram is broken or not by cutting it. Typical diagrams involving one-impurity processes are illustrated in Fig. 1 and 2 in the next section.

3. One-impurity interaction diagrams

Let us consider the arbitrarily case of strong coupling in which electrons interact so strongly with impurities of a low density n_s that the contribution of the higher order processes in the strength of the interaction must be considered.

Since we are dealing with dilute impurity system, only those diagrams for g_z and $(f_z n')^{(c)}$ in which all the potential bonds terminate at the same common impurity center

will be enumerated. These diagrams are shown in Fig. 1 and 2. Their contributions are given by

$$g_z = g_z^{(1)} + g_z^{(2)} + g_z^{(3)} + \dots \tag{3.1}$$

$$(f_z n')^{(c)} = (f_z n')^{(c,1)} + (f_z n')^{(c,2)} + \dots, \tag{3.2}$$

where the upper numerals denote the numbers of the potential bonds.

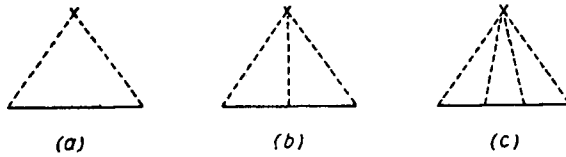


Fig. 1. Diagrams representing $g_z^{(2)}$, $g_z^{(3)}$ and $g_z^{(4)}$

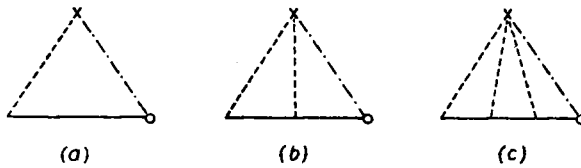


Fig. 2. Diagrams representing $(f_z n')^{(c,1)}$, $(f_z n')^{(c,2)}$ and $(f_z n')^{(c,3)}$

The practical calculation of these terms in Landau representation may be facilitated by the use of $\nu-\mu$ representation.

Let us specify the $\nu_1-\nu_2$ element of an arbitrary operator A by

$$\langle \nu_1 | A | \nu_2 \rangle \equiv A_{\nu_1-\nu_2} \left(\frac{\nu_1 + \nu_2}{2} \right). \tag{3.3}$$

If we introduce a pair of variables (ν, μ) replacing the pair (ν_1, ν_2) such that

$$\nu \equiv \frac{\nu_1 + \nu_2}{2} \quad \mu \equiv \nu_1 - \nu_2, \tag{3.4}$$

we may express (3.3) as

$$A_\mu(\nu) = \left\langle \nu + \frac{1}{2} \mu | A | \nu - \frac{1}{2} \mu \right\rangle. \tag{3.5}$$

Let us define a linear operator $h(\nu)$ whose $\mu-\mu'$ element is given by

$$\langle \mu | h(\nu) | \mu' \rangle \equiv \eta^{\mu'} h_{\mu-\mu'}(\nu) \eta^{-\mu} - \eta^{-\mu'} h_{\mu-\mu'}(\nu) \eta^\mu, \tag{3.6}$$

where $\eta^{\pm\mu}$ are displacement operators which upon acting on a function Φ of ν yield

$$\eta^{\pm\mu} \Phi(\nu) = \Phi \left(\nu \pm \frac{1}{2} \mu \right) \eta^{\pm\mu}. \tag{3.7}$$

It can be verified that the operators h and $h(\nu)$ are related by

$$\left\langle \nu + \frac{1}{2} \mu | h A | \nu - \frac{1}{2} \mu \right\rangle = \sum_{\mu'} (\mu | h(\nu) | \mu') A_{\mu'}(\nu). \quad (3.8)$$

From (3.6) one can obtain

$$\begin{aligned} (\mu | h_0(\nu) | \mu') &= (\varepsilon_{\nu+\frac{1}{2}\mu} - \varepsilon_{\nu-\frac{1}{2}\mu}) \delta_{\mu, \mu'} \\ (\mu | v(\nu) | \mu') &= \sum_{\alpha} (\mu | \tilde{v}_{\alpha}(\nu) | \mu') \\ &= \left\langle \nu + \frac{1}{2} \mu | v | \nu + \mu' - \frac{1}{2} \mu \right\rangle \eta^{\mu' - \mu} - \left\langle \nu - \mu' + \frac{1}{2} \mu | v | \nu - \frac{1}{2} \mu \right\rangle \eta^{-\mu' + \mu}. \end{aligned} \quad (3.9)$$

As an illustrating example, we calculate the $\nu_1 - \nu_2$ element of $g_z^{(2)}\psi$ (Fig. 1a) in this representation.

$$\begin{aligned} \langle \nu_1 | g_z^{(2)} \psi | \nu_2 \rangle &= \sum_{\mu_s} (\mu | g_z^{(2)}(\nu) | \mu_s) \psi_{\mu_s}(\nu) \\ &= (2\pi)^3 n_s (-\lambda)^2 \sum_{\mu_1, \mu_2} (\mu | \tilde{v}(\nu) | \mu_1) \left(\mu_1 \left| \frac{1}{h_0(\nu) - z} \right| \mu_1 \right) (\mu_1 | \tilde{v}(\nu) | \mu_2) \psi_{\mu_s}(\nu) \\ &= (2\pi)^3 n_s (-\lambda)^2 \sum_{\mu_1, \mu_2} \left\{ \left\langle \nu + \frac{1}{2} \mu | \tilde{v} | \nu + \mu_1 - \frac{1}{2} \mu \right\rangle (\varepsilon_{\nu + \mu_1 + \frac{1}{2} \mu} - \varepsilon_{\nu - \frac{1}{2} \mu} - z)^{-1} \times \right. \\ &\quad \times \left[\left\langle \nu + \mu_1 - \frac{1}{2} \mu | \tilde{v} | (\nu + \mu_2 - \frac{1}{2} \mu) \right\rangle \psi_{\mu_s} \left(\nu + \frac{1}{2} \mu_2 - \frac{1}{2} \mu \right) - \right. \\ &\quad \left. \left. - \left\langle \nu + \mu_1 - \mu_2 - \frac{1}{2} \mu | \tilde{v} | \nu - \frac{1}{2} \mu \right\rangle \psi_{\mu_s} \left(\nu + \mu_1 - \frac{1}{2} \mu_2 - \frac{1}{2} \mu \right) \right] + \right. \\ &\quad \left. + \left\langle \nu - \mu_1 + \frac{1}{2} \mu | \tilde{v} | \nu - \frac{1}{2} \mu \right\rangle (\varepsilon_{\nu + \frac{1}{2} \mu} - \varepsilon_{\nu - \mu_1 + \frac{1}{2} \mu} - z)^{-1} \times \right. \\ &\quad \times \left[\left\langle \nu - \mu_2 + \frac{1}{2} \mu | \tilde{v} | \nu - \mu_1 + \frac{1}{2} \mu \right\rangle \psi_{\mu_s} \left(\nu + \frac{1}{2} \mu - \frac{1}{2} \mu_2 \right) - \right. \\ &\quad \left. \left. - \left\langle \nu + \frac{1}{2} \mu | \tilde{v} | \nu + \mu_2 - \mu_1 + \frac{1}{2} \mu \right\rangle \psi_{\mu_s} \left(\nu - \mu_1 + \frac{1}{2} \mu_2 + \frac{1}{2} \mu \right) \right] \right\} \\ &= (2\pi)^3 n_s (-\lambda)^2 \sum_{\nu_1, \nu_2} \{ \langle 1 | \tilde{v} | 3 \rangle (\varepsilon_3 - \varepsilon_2 - z)^{-1} \times [\langle 3 | \tilde{v} | 4 \rangle \langle 4 | \psi | 2 \rangle - \langle 4 | \tilde{v} | 2 \rangle \langle 3 | \psi | 4 \rangle] + \\ &\quad + \langle 3 | \tilde{v} | 2 \rangle (\varepsilon_1 - \varepsilon_3 - z)^{-1} \times [\langle 4 | \tilde{v} | 3 \rangle \langle 1 | \psi | 4 \rangle - \langle 1 | \tilde{v} | 4 \rangle \langle 4 | \psi | 3 \rangle] \}. \end{aligned} \quad (3.10)$$

4. Analysis of o -diagrams in terms of c -diagrams

In the actual evaluation of matrix elements, the technique of $\nu - \mu$ representation described in the previous section is useful. However, this technique leads to the introduction of displacement operators η , see (3.6). While the displacement by itself is a straightforward

operation, its repetition becomes increasingly laborious for higher order calculation. It is found possible to obtain the operated-out expressions directly by introducing another kind of diagrams, which represent ordinary quantum operators rather than the products of Liouville operators and ordinary operators.

The diagrams employed so far in the previous sections will be called *o-diagrams* for the sake of distinction.

We define *c-diagrams* such that they can be generated from *o-diagrams* in the following way:

- i. Draw a horizontal boundary line, which divides the whole plane into two half-planes.
- ii. Draw two solid horizontal (electron) lines, one above and the other below the boundary line. They are joined together by a vertical solid line at the right end.
- iii. Corresponding to an *o*-diagram of k -th order, mark k vertices by distributing them, in 2^k ways, on the upper and/or lower solid lines without changing the left-to-right positions and the structure of potential bonds.

Thus, an *o*-diagram of k -th order generates the number 2^k of similar *c*-diagrams. The four *c*-diagrams generated by the *o*-diagram in Fig. 1a are drawn in Fig. 3.

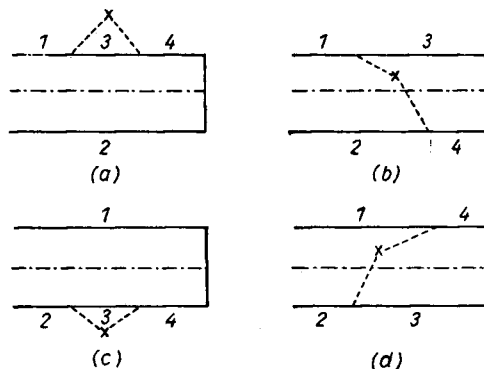


Fig. 3. The *c*-diagrams generated by the second order *o*-diagram in Fig. 1a correspond to the four terms of the last member of (3.10)

It is noted that the four terms in (3.10) can be read directly from these four *c*-diagrams.

(i) Each particle line segment between successive potential vertices or between a vertex and the intersection of the vertical line with the boundary is given an electronic state. Corresponding to a vertex on the upper line, associate a matrix element of $(-\lambda\tilde{v})$ between two neighbouring states from left to right as they appear in the diagram, while corresponding to that on the lower line a matrix element of $(+\lambda\tilde{v})$ between two states in the reverse order (from right to left).

(ii) By following the vertical line down the matrix element of ψ can be read.

(iii) Corresponding to a parallel layer whose boundaries are the (imagined) vertical straight lines cutting through two vertices, associate a factor $(\epsilon_{jk}-z)^{-1} \equiv [\epsilon_j - \epsilon_k - z]^{-1}$ where j and k are respectively those states read from the upper and lower particle lines within the layer.

(iv) Sum with respect to all state variables except for ν_1 and ν_2 .

(v) Multiply the whole expression by $(2\pi)^3 n_3$.

These rules are not restricted to this particular case. They are valid for all diagrams in $g_x \psi$.

In the case of $(f_z n')^{(c)}$, the matrix element of n' is read in the same way as that of ψ in the rule (ii).

5. Summation of diagrams

Let us consider the collection of those o -diagrams for $g_x \psi$ which correspond to one-electron-one-impurity processes. We shall analyze the collection in terms of the associated c -diagrams. Any c -diagram can be classified into either class 'x' or class 'y' according to whether the vertex at the far left lies above or below the boundary.

Let us first consider the class x . Those diagrams in x which have all vertices on the upper line are drawn in Fig. 4, where we omit the potential bonds and represent the vertices by white circles.

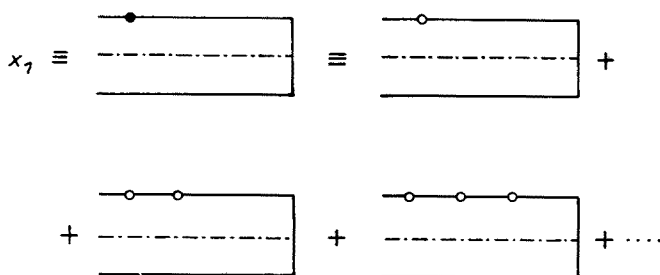


Fig. 4. Diagrams representing the subclass x_1

The contribution of these diagrams can be easily evaluated by using the rules given in Section 4. It is given by

$$(x_1)_{\nu\nu'} = (2\pi)^3 n_3 \left\{ - \sum_{\nu_1} \lambda \tilde{v}_{\nu_1} \psi_{1\nu'} + \sum_{\nu_1, \nu_2} \lambda^2 \tilde{v}_{\nu_1} (\varepsilon_{1\nu'} - z)^{-1} \tilde{v}_{12} \psi_{2\nu'} - \sum_{\nu_1, \nu_2, \nu_3} \lambda^3 \tilde{v}_{\nu_1} (\varepsilon_{1\nu'} - z)^{-1} \tilde{v}_{12} (\varepsilon_{2\nu'} - z)^{-1} \tilde{v}_{23} \psi_{3\nu'} + \dots \right\}. \quad (5.1)$$

By introducing an operator $t(\nu)$, which is defined by

$$t(\nu)_{12} = \lambda \tilde{v}_{12} - \sum_{\nu_3, \nu_4} \lambda \tilde{v}_{13} [h_0(\nu) - z]_{34}^{-1} t(\nu)_{42} \equiv \lambda \tilde{v}_{12} - \sum_{\nu_3, \nu_4} \lambda \tilde{v}_{13} d(\nu)_{34} t(\nu)_{42} \quad (5.2)$$

$$h_0(\nu)_{12} \equiv \varepsilon_{1\nu} \delta_{12} \equiv (\varepsilon_1 - \varepsilon_\nu) \delta_{12}. \quad (5.3)$$

$$d(\nu) \equiv [h_0(\nu) - z]^{-1}, \quad (5.4)$$

we can rewrite (5.1) as

$$(x_1)_{\nu\nu'} = -(2\pi)^3 n_3 \sum_{\nu_1} t(\nu')_{\nu_1} \psi_{1\nu'}. \quad (5.5)$$

It is noted that (5.5) can be obtained from the contribution of the first-order diagram by replaced v with $t(v')$. We denote the sum of the diagrams in x_1 by the diagram marked with a black circle on the upper line.

Let us now consider the subclass x_2 (see Fig. 5) each of whose element has the all vertices on the upper line standing to the left of the all vertices on the lower line.

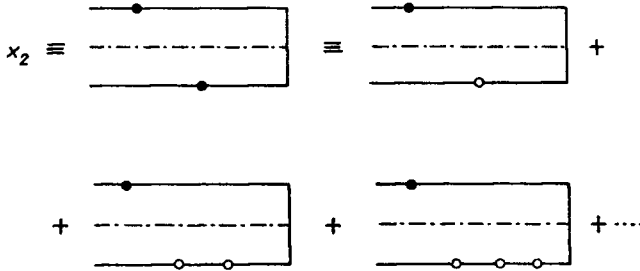


Fig. 5. Diagrams representing the subclass x_2

Its contribution is given by

$$\begin{aligned}
 (x_2)_{v,v'} &= -(2\pi)^3 n_s \{ \lambda \sum_{v_1, v_2} t(v')_{v_1} \psi_{12} \tilde{v}_{2v'} (\epsilon_{1v'} - z)^{-1} + \lambda^2 \sum_{v_1, v_2, v_3} t(v')_{v_1} \psi_{12} \tilde{v}_{23} (\epsilon_{13} - z)^{-1} \tilde{v}_{3v'} (\epsilon_{1v'} - z)^{-1} + \dots \} \\
 &= -(2\pi)^3 n_s \sum_{v_1, v_2} [t(v') d(v')]_{v_1} \psi_{12} t^*(1)_{2v'}, \tag{5.6}
 \end{aligned}$$

where

$$t^*(v) \equiv \lambda \tilde{v} - \lambda \tilde{v} d^*(v) t^*(v) \tag{5.7}$$

$$d^*(v) \equiv [h_0(v) + z]^{-1}. \tag{5.8}$$

It is seen that the expression (5.6) can be obtained directly by inspecting the diagram marked with two black circles by applying the same rules for the corresponding diagram with white circles except for replacing v 's with t and t^* , the argument of which being read by looking at the state of the particle line at the opposite side of the black circle with respect to the boundary.

It is clear that the total collection x may be obtained by summing x_1, x_2, \dots , shown in Fig. 6, those diagrams marked with one, two, black circles distributed alternatively across the boundary.

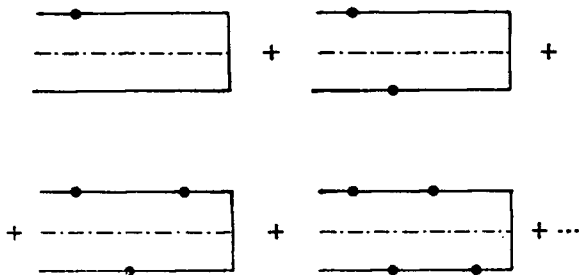


Fig. 6. Collection of diagrams for the class x

The contribution of x can be written down as

$$\begin{aligned} \frac{x_{\nu\nu'}}{(2\pi)^3 n_s} = & - \sum_{\nu_1} t(\nu')_{\nu_1} \psi_{1\nu'} - \sum_{\nu_1, \nu_2} [t(\nu')d(\nu')]_{\nu_1} \psi_{12} t^*(1)_{2\nu'} - \\ & - \sum_{\nu_1, \nu_2, \nu_3} [t(\nu')d(\nu')]_{\nu_1} t(3)_{12} \psi_{23} [d^*(1)t^*(1)]_{3\nu'} - \\ & - \sum_{\nu_1, \nu_2, \nu_3, \nu_4} [t(\nu')d(\nu')]_{\nu_1} [t(4)d(4)]_{12} \psi_{23} t^*(2)_{34} [d^*(1)t^*(1)]_{4\nu'} \dots \end{aligned} \quad (5.9)$$

This infinite series can be expressed as the solution of the following integral equation,

$$\begin{aligned} x_{\nu\nu'} = & -(2\pi)^3 n_s \left\{ \sum_{\nu_1} t(\nu')_{\nu_1} \psi_{1\nu'} + \sum_{\nu_1, \nu_2} [t(\nu')d(\nu')]_{\nu_1} \psi_{12} t^*(1)_{2\nu'} \right\} + \\ & + \sum_{\nu_1, \nu_2} [t(\nu')d(\nu')]_{\nu_1} x_{12} [d^*(1)t^*(1)]_{2\nu'}. \end{aligned} \quad (5.10)$$

In a similar manner we can evaluate the contribution of class y . The result can be written as the solution of the integral equation,

$$\begin{aligned} y_{\nu\nu'} = & (2\pi)^3 n_s \left\{ \sum_{\nu_1} \psi_{\nu_1} t^*(\nu)_{1\nu'} + \sum_{\nu_1, \nu_2} t(2)_{\nu_1} \psi_{12} [d^*(\nu)t^*(\nu)]_{2\nu'} \right\} + \\ & + \sum_{\nu_1, \nu_2} [t(2)d(2)]_{\nu_1} y_{12} [d^*(\nu)t^*(\nu)]_{2\nu'}. \end{aligned} \quad (5.11)$$

The contribution of one-impurity process to the field term $\left(f_z \frac{\partial n'}{\partial u} \right)^{(c)}$ can be similarly calculated. This contribution is also written as the sum of two terms 'X' and 'Y', which correspond to the analogous division of 'x' and 'y' in the case of the collision term $g_z \psi \cdot X_{\nu\nu'}$ and $Y_{\nu\nu'}$ are given by the solutions of the following integral equations,

$$\begin{aligned} X_{\nu\nu'} = & (2\pi)^3 n_s \left\{ - \sum_{\nu_1} [t(\nu')d(\nu')]_{\nu_1} \left(\frac{\partial n'}{\partial u} \right)_{1\nu'} + \sum_{\nu_1, \nu_2} [t(\nu')d(\nu')]_{\nu_1} \left(\frac{\partial n'}{\partial u} \right)_{12} [d^*(1)t^*(1)]_{2\nu'} \right\} + \\ & + \sum_{\nu_1, \nu_2} [t(\nu')d(\nu')]_{\nu_1} X_{12} [d^*(1)t^*(1)]_{2\nu'}. \end{aligned} \quad (5.12)$$

$$\begin{aligned} Y_{\nu\nu'} = & (2\pi)^3 n_s \left\{ \sum_{\nu_1} \left(\frac{\partial n'}{\partial u} \right)_{\nu_1} [d^*(\nu)t^*(\nu)]_{1\nu'} + \sum_{\nu_1, \nu_2} [t(2)d(2)]_{\nu_1} \left(\frac{\partial n'}{\partial u} \right)_{12} [d^*(\nu)t^*(\nu)]_{2\nu'} + \right. \\ & \left. + \sum_{\nu_1, \nu_2} [t(2)d(2)]_{\nu_1} Y_{12} [d^*(\nu)t^*(\nu)]_{2\nu'}. \right. \end{aligned} \quad (5.13)$$

In summary, the contribution to the collision and field terms are given respectively by

$$\begin{aligned} g_z \psi = & x + y \\ \left(f_z \frac{\partial n'}{\partial u} \right)^{(c)} = & X + Y. \end{aligned} \quad (5.14)$$

It is seen from (5.10—5.13) that the operators on the right hand side can be completely described in terms of the generalizations (t, t^*) , in (5.2) and (5.7), of the conventional

transition matrix T , which is defined by [6]

$$T(v)_{12} = \lambda \tilde{v}_{12} - \sum_{v_3} \lambda \tilde{v}_{13} [\varepsilon_3 - \varepsilon_v - ia]^{-1} T(v)_{32}. \quad (5.15)$$

The present analysis of one-impurity process can be applied to the system subjected to a constant magnetic field B as well as to the field-free system. In the absence of the magnetic field, the use of the momentum representation greatly simplifies the present formulation. We shall discuss this and other aspects in a forthcoming paper.

One of the authors (S.F) wishes to thank Professors Charles A. Randall and E. Breitenberger for the hospitality during his stay at the Ohio University where the main part of the manuscript was written.

REFERENCES

- [1] C. C. Chen and S. Fujita, *J. Phys. Chem. Solids*, **28**, 607 (1967).
- [2] S. Fujita, *J. Phys. Chem. Solids*, **28**, 615 (1967); S. Fujita and Fuliński, *Acta Phys. Polon.*, **29**, 679 (1966).
- [3] R. Kubo, *J. Phys. Soc. Japan*, **12**, 570 (1957).
- [4] J. M. Luttinger and W. Kohn, *Phys. Rev.*, **109**, 1892 (1958); S. F. Edwards, *Phil. Mag.*, **3**, 1021 (1958).
- [5] S. Fujita, *Introduction to Non-Equilibrium Quantum Statistical Mechanics*, W. B. Saunders, Philadelphia 1966.
- [6] E. Merzbacher, *Quantum Mechanics*, John Wiley, New York 1961.